

# Bayesian inference of epidemics on networks via Belief Propagation

Fabrizio Altarelli,<sup>1,2</sup> Alfredo Braunstein,<sup>1,3,2</sup> Luca Dall'Asta,<sup>1,2</sup>  
Alejandro Lage-Castellanos,<sup>1,4</sup> and Riccardo Zecchina<sup>1,3,2</sup>

<sup>1</sup>*DISAT and Center for Computational Sciences, Politecnico di Torino,  
Corso Duca degli Abruzzi 24, 10129 Torino, Italy*

<sup>2</sup>*Collegio Carlo Alberto, Via Real Collegio 30, 10024 Moncalieri, Italy*

<sup>3</sup>*Human Genetics Foundation, Via Nizza 52, 10126 Torino, Italy*

<sup>4</sup>*Physics Faculty, Havana University, San Lazaro y L, 10400 Habana, Cuba*

We study several bayesian inference problems for irreversible stochastic epidemic models on networks from a statistical physics viewpoint. We derive equations which allow to accurately compute the posterior distribution of the time evolution of the state of each node given some observations. At difference with most existing methods, we allow very general observation models, including unobserved nodes, state observations made at different or unknown times, and observations of infection times, possibly mixed together. Our method, which is based on the Belief Propagation algorithm, is efficient, naturally distributed, and exact on trees. As a particular case, we consider the problem of finding the “zero patient” of a SIR or SI epidemic given a snapshot of the state of the network at a later unknown time. Numerical simulations show that our method outperforms previous ones on both synthetic and real networks, in some cases by a very large margin.

Tracing epidemic outbreaks in order to pin down where they came from is one of the paramount problem in epidemiology. Compared to the pioneering work of John Snow on 1854 London’s cholera hit [1], modern computational epidemiology has more accurate clinical data and can employ powerful computers to run large-scale simulations of stochastic compartment models, but finding the origin or *seed* of an epidemic outbreak, like most *inverse* epidemic problems, remains a very challenging problem.

Even for simple stochastic epidemic models such as the susceptible-infected (SI) and the susceptible-infected-recovered (SIR) model, finding the most likely origin of an observed epidemic outbreak is still an open and difficult computational problem. In recent years several studies proposed maximum likelihood estimators of various kinds, including estimators for acyclic graphs, in particular for regular trees [2] or under strong simplifying assumptions on the spreading process [3]. Most proposed estimators are based either on topological centrality measures [2] or on measures of the distance between observed data and the typical outcome of propagations from given initial conditions [4]. Among recently proposed methods, Dynamic Message Passing (DMP) [5] is particularly interesting as it addresses the problem more systematically, directly attempting to approximate and maximize the likelihood function. DMP makes use of a statistical physics-inspired formulation of the dynamic evolution of the stochastic process [6] which is at the same time very accurate in providing local probability marginals and extremely efficient even on large graphs. Then it estimates the likelihood of any given initial condition by means of an additional single-site factorization approximation of the likelihood function. Despite its appeal, and as noted by the authors, this method has two drawbacks. First, the space of initial conditions considered must be small, because it must be explored exhaustively. Second, it relies on a single-site factorization of the likelihood function which is not necessarily consistent with the more accurate underlying approximation in [6].

In this Letter we derive the Belief Propagation (BP) equations for the posterior distribution of past states conditioned on some observations made at a later time, without additional hypotheses. In contrast with DMP, the expression we obtain for the posterior distribution is exact on acyclic graphs, and will be shown to be a typically better approximation on general graphs. The method can be used to identify the origin of an epidemic outbreak in the SIR, SI, and similar models, even with multiple infection sources and incomplete information.

## I. THE SIR MODEL ON GRAPHS.

The susceptible-infected-recovered (SIR) model of spreading is a stochastic dynamical model in discrete time defined over a graph  $G = (V, E)$ . At time  $t$  a node  $i$  can be in one of three states (*infected*, *susceptible* or *recovered*) represented by a variable  $x_i^t \in \{S, I, R\}$ . The dynamical process is defined as follows: at each time step  $t$ , each node  $i$  in the infected state attempts to infect each one of its susceptible neighbors  $\{j \in \partial i : x_j^t = S\}$ , succeeding with independent probabilities  $\lambda_{ij} \in [0, 1]$ ; then, node  $i$  attempts to recover, succeeding with probability  $\mu_i \in [0, 1]$ . The dynamics is clearly irreversible, as a given node can only undergo the transitions  $S \rightarrow I \rightarrow R$ , and thus a stationary condition will be reached in finite time (with all nodes either in the  $S$  or  $R$  state provided  $\mu_i > 0$ ). Two important special cases of SIR are: **(a)** the Independent Cascade (IC) model, obtained when  $\mu_i \equiv 1$ , which has been extensively studied in the

related context of optimization of the spread of information [7]. The case with  $\lambda_{ij} \equiv 1$  is a simple percolation process. **(b)** the susceptible-infected (SI) model, obtained when  $\mu_i \equiv 0$ .

## II. SIR DYNAMICS AS A GRAPHICAL MODEL AND BAYESIAN INFERENCE.

Assume that a certain set of nodes initiates the infection at time  $t = 0$ , i.e. with  $x_i^0 = I$ . With respect to this initial set, a realization of the SIR process can be univocally expressed in terms of a set of *recovery times*  $g_i$  (i.e. the time-lag after which node  $i$  recovers if it gets infected) and of *transmission delays*  $s_{ij}$  (a time-lapse between the infection of  $i$  and a potential first successful transmission event from  $i$  to  $j$ ). The infection times  $t_i$  can be deterministically computed by imposing the condition  $1 = \phi_i = \delta(t_i, \mathbb{1}[x_i^0 \neq I] (\min_{j \in \partial i} \{t_j + s_{ji}\} + 1))$  for every  $i$ . The recovery times  $g_i$  are independent and drawn from geometric distributions  $\mathcal{G}_i(g_i) = \mu_i (1 - \mu_i)^{g_i}$ , while the transmission delays  $s_{ij}$  are independent and follow geometric distributions truncated at  $g_i$ , i.e.  $\omega_{ij}(s_{ij}|g_i) = \lambda_{ij} (1 - \lambda_{ij})^{s_{ij}}$  for  $s_{ij} \leq g_i$  and  $\omega_{ij}(\infty|g_i) = \sum_{s > g_i} \lambda_{ij} (1 - \lambda_{ij})^s$ . The distribution of infection and recovery times  $\mathbf{t}, \mathbf{g}$  given the initial state  $\mathbf{x}^0$  can be written as

$$\begin{aligned} \mathcal{P}(\mathbf{t}, \mathbf{g} | \mathbf{x}^0) &= \sum_{\mathbf{s}} \mathcal{P}(\mathbf{s} | \mathbf{g}) \mathcal{P}(\mathbf{t} | \mathbf{x}^0, \mathbf{g}, \mathbf{s}) \mathcal{P}(\mathbf{g}) \\ &= \sum_{\mathbf{s}} \prod_{i,j} \omega_{ij} \prod_i \phi_i \mathcal{G}_i. \end{aligned} \quad (1)$$

In the inference problem, we assume (i) to know the state of an epidemic at time  $t = T$ , i.e. the state of every node  $x_i^T \in \{S, I, R\}$ , and (ii) to possess only probabilistic prior information about the set of initially infected nodes, represented by a factorized *a priori* distribution  $\mathcal{P}(\mathbf{x}^0) = \prod_i \gamma_i(x_i^0)$  of initial infection. Using Bayes' theorem, the posterior distribution can be expressed as

$$\begin{aligned} \mathcal{P}(\mathbf{x}^0 | \mathbf{x}^T) &\propto \sum_{\mathbf{t}, \mathbf{g}} \mathcal{P}(\mathbf{x}^T | \mathbf{t}, \mathbf{g}) \mathcal{P}(\mathbf{t}, \mathbf{g} | \mathbf{x}^0) \mathcal{P}(\mathbf{x}^0) \\ &= \sum_{\mathbf{t}, \mathbf{g}, \mathbf{s}} \prod_{i,j} \omega_{ij} \prod_i \phi_i \mathcal{G}_i \gamma_i \zeta_i \end{aligned} \quad (2)$$

where we exploited the fact that the state  $\mathbf{x}^T$  at time  $T$  given a set  $(\mathbf{t}, \mathbf{g})$  of infection and recovery times follows a deterministic law  $\mathcal{P}(\mathbf{x}^T | \mathbf{t}, \mathbf{g}) = \prod_i \zeta_i(t_i, g_i, x_i^T)$  where  $\zeta_i = \mathbb{1}[x_i^T = I, t_i \leq T < t_i + g_i] + \mathbb{1}[x_i^T = S, t_i < T] + \mathbb{1}[x_i^T = R, t_i + g_i \leq T]$ .

## III. BELIEF PROPAGATION EQUATIONS FOR THE LIKELIHOOD FUNCTION.

Finding the marginals of the effective model (2) is computationally intractable in the worst case, and so we propose to perform this calculation approximately using Belief Propagation. For this purpose we will use the Factor graph terminology (borrowed from graphical models) i.e. the bipartite graph of dependence of factors in a generalized Boltzmann weight and their variables. Since every constraint  $\phi_i$  contains terms of the type  $t_j + s_{ji}$ , it is more convenient to introduce new variables  $t'_j = t_j + s_{ji}$  and eliminate the  $s_{ij}$  and  $s_{ji}$  parameters from the graphical model. Defining factors  $\phi_{ij} = \omega_{ij}(t'_i - t_i | g_i) \omega_{ji}(t'_j - t_j | g_j)$  and  $\phi_i = \delta(t_i, \mathbb{1}[x_i^0 \neq I] (\min_{j \in \partial i} \{t'_j\} + 1))$ , the posterior probability becomes  $\mathcal{P}(\mathbf{x}^0 | \mathbf{x}^T) \propto \sum_{\mathbf{t}, \mathbf{t}', \mathbf{g}} \prod_{i < j} \phi_{ij} \prod_i \phi_i \mathcal{G}_i \gamma_i \zeta_i$ . Note that even in a simplistic deterministic scenario with  $\mu_i \equiv \lambda_{ij} \equiv 1$  and thus  $t'_i = t_i$ , the graphical model corresponding to factors  $\phi_i$  has the loopy factor graph representation displayed in Fig.1b (see also [8]). The representation can be disentangled by grouping pairs of activation times  $(t_i, t_j)$  in the same variable (see Fig.1c), which is crucial to make the approximation more accurate, and exact on trees. Similarly for the general case (2), we define set of dynamical variables given by triplets  $(g_i^{(j)}, t_i^{(j)}, t'_j)$  and regroup dynamical constraint with compatibility checks into the factor node  $\psi_i = \phi_i(t_i, \mathbf{t}_{\partial i}^0) \prod_{j \in \partial i} \delta(t_i^{(j)}, t_i) \delta(g_i^{(j)}, g_i)$  (See Fig. 1d). We obtain an *effective* model

$$\mathcal{Q} = \frac{1}{Z} \prod_{i < j} \phi_{ij} \prod_i \psi_i \mathcal{G}_i \gamma_i \zeta_i \quad (3)$$

in terms of which  $\mathcal{P}(\mathbf{x}^0 | \mathbf{x}^T) \propto \sum_{\mathbf{t}, \mathbf{t}', \mathbf{g}} \mathcal{Q}(\mathbf{g}, \mathbf{t}, \mathbf{t}', \mathbf{x}^0)$ . As the topology of the constructed factor graph mirrors the one of the original network, this approach allows the exact computation of posterior marginals for the SIR model on tree graphs.

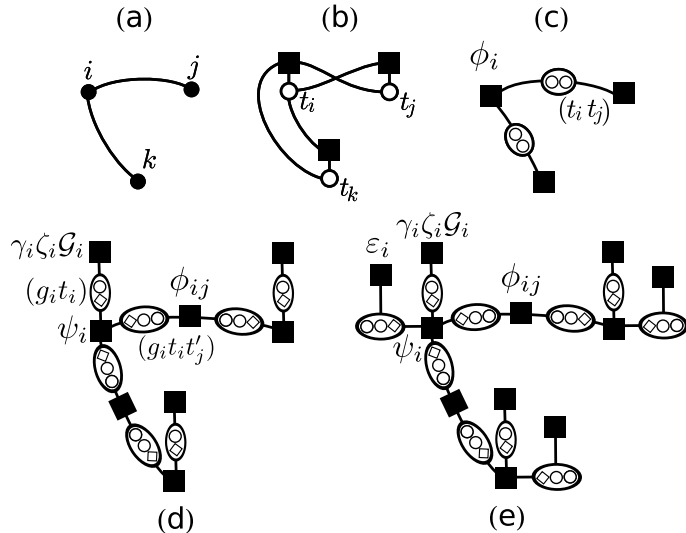


Figure 1. Factor graph representations for irreversible dynamics: squares represent factors of a generalized Boltzman distribution and connected circles the variables on which they depend. (a) Original graph (b) Loopy, naive factor graph for an irreversible deterministic dynamics (c) Disentangled dual tree factor graph (d) Factor graph for the SIR model given in (3) with known epidemic age (e) Factor graph representation with unknown epidemic age.

Belief propagation equations can be written for the efficient approximate computation of marginals of (3) (See SM). The BP update of  $\psi_i$  can be computed in time  $O(G \cdot T \cdot |\partial i|)$ , where  $G$  is the maximum allowed recovery delay, and the one of  $\phi_{ij}$  in time  $O(G^2 \cdot T)$ . In practice,  $G$  can be taken constant for a geometric distribution  $\mathcal{G}$ . A single BP iteration can be thus computed in time  $O(T \cdot G^2 \cdot |E|)$ . Once the BP equations converge, estimates for the infection time  $t_i$  of each node are obtained, and nodes can be ranked by the posterior probability of being a seed of the epidemics  $\mathcal{P}(x_i^0 = I | \mathbf{x}^T)$ .

#### IV. IDENTIFICATION OF A SINGLE SOURCE.

In the following we restrict ourselves to random regular graphs of degree  $k = 4$  and  $N = 1000$  nodes with homogeneous propagation probability  $\lambda_{ij} \equiv \lambda$  and recovery probability  $\mu_i \equiv \mu$  in order to make comparison with other inference methods simpler. We compared the inference performance of BP with the one of DMP. Given a starting condition, the DMP method iterates the forward probabilistic transmission equations of [6] to obtain single-site trajectory probability distributions. Afterwards, using a single-site factorization hypothesis for the joint distribution at the observation time, it gives a simple factorized expression of the likelihood of the initial condition that can be computed. This procedure has to be repeated for each possible initial condition considered, and the one with largest likelihood is selected. DMP is shown in [5] to outperform other more classical, topology-based, estimations of the epidemic origin [2]. We found that DMP can be improved over its original presentation if the dynamic MP equations are not iterated over all nodes of the graph, but only over the part of the graph that is involved in the epidemic. We refer to this version as DMP-restricted or DMP<sub>r</sub> (see SM for details). Besides DMP and DMP<sub>r</sub>, we tested the performance of the Jordan centrality method [2].

We generated  $10^3$  instances with observation time  $T = 10$  and recovery probability  $\mu = 0.5$ , for variable values of transmission probability  $\lambda$ . In Figure 2 (a) we show the fraction of instances in which the true zero patient was found by BP, DMP, DMP<sub>r</sub> and Jordan centrality vs. the average size of the epidemic for each  $\lambda$ . Since DMP requires a defined value of the observation time, we here assume that  $T = 10$  is known for DMP, DMP<sub>r</sub> and BP. BP outperforms DMP by a large margin in the probability of finding the epidemic origin. We computed for each case the normalized ranking  $(\text{rank } i_0)/|G_0|$  where  $|G_0|$  is the number of infected plus recovered individuals. Panel (b) shows also a remarkable difference in the normalized ranking of the true origin given by all three algorithms, again BP outperforming the other three.

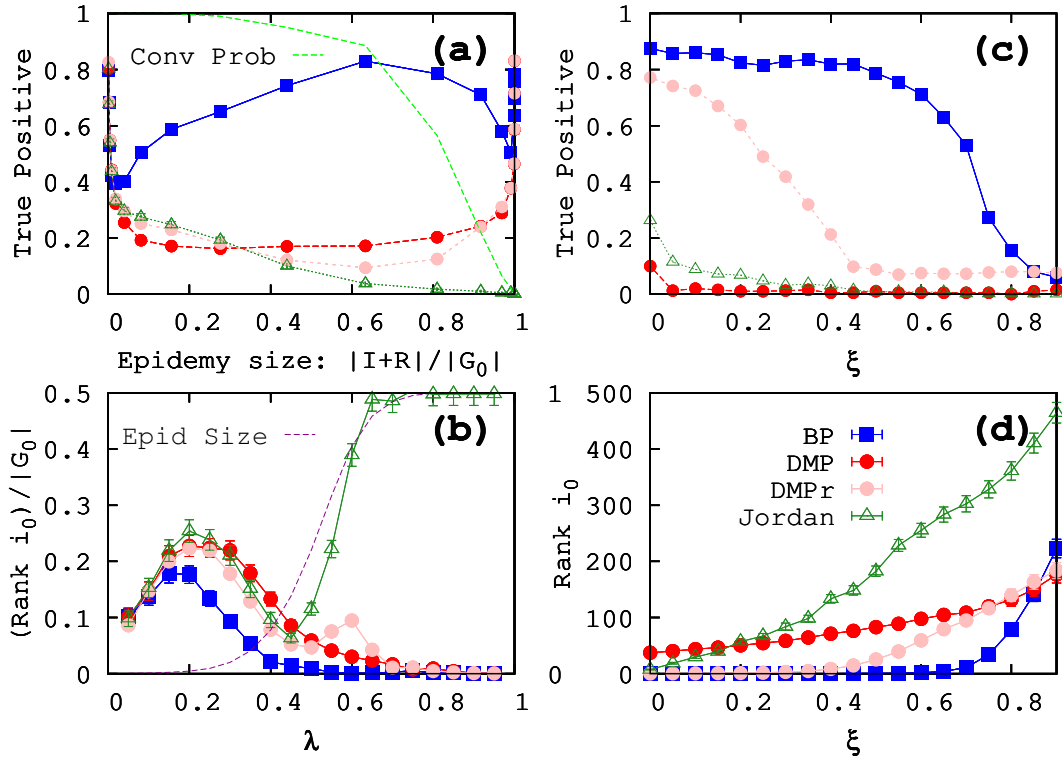


Figure 2. Comparison of Jordan, DMP, DMPr and BP methods on RRG with  $N = 1000, k = 4$  with observation time  $T = 10$ . Points are averages over  $10^3$  instances. (a) Probability of finding the true origin of the epidemic as a function of the average epidemic size ( $\mu = 0.5$ ) (b) Normalized rank given to the true zero patient  $i_0$ , as a function of the transmission probability  $\lambda$ , for the same cases as in (a). The epidemic size is also plotted (purple, right axis). For too large epidemic BP may fail to converge within the specified number of iterations (convergence probability: green in (a)), but relevant information is still present in the (unconverged) marginals. (c) Probability of finding the true origin of the epidemic as a function of  $\xi$ . Recovery probability was  $\mu = 1$  and transmission probability was  $\lambda = 0.5$ . (d) Absolute rank given by each algorithm to the true zero patient as a function of the fraction  $\xi$  of the graph that is unobserved.

## V. INCOMPLETE INFORMATION.

In a more realistic setup, much of the information we assumed to know can be missing. First, only a fraction of the nodes can usually be observed. Calling  $\xi$  the fraction of unobserved nodes (we denote  $X$  the unknown state), we computed the average ranking given to the real zero patient by BP, and compared it with other three methods in Fig. 2 (c,d). In the case of restricted DMP, the unobserved nodes are obviously taken into account for the dynamic message passing. More precisely, only the connected component of  $I, R$  and  $X$  nodes is used for the DMPr method (see SM). Jordan centrality is also computed over this connected component as in [5]. BP is quite efficient in this regime, finding the true zero patient in more than 70% of instances up to 60% of unobserved sites (panel (c)), and outperforming the other methods for almost all  $\xi$ .

Second, the initial time  $T_0$  of the epidemic could be unknown. Starting with an upper bound on the epidemic duration, it suffices to consider the dynamical process to start from the all-susceptible state but to allow nodes to be spontaneously infected at an arbitrary time with (small) uniform probability. This is equivalent to the addition of a fictitious virtual neighbor to every node with no constraint  $\psi_i$  in its activation time but with a prior probability  $\varepsilon_i(g_i'', t_i'', t_i) = \delta(t_i'', \infty)(1 - 2\gamma) + \gamma$  of spontaneous infection (See Fig. 1e). An example of inference for an epidemic with recovery and transmission probabilities  $\lambda = 0.7, \mu = 0.6$  is depicted in Fig. 3 in which only a fraction 0.6 of the nodes was observed and the origin time is unknown. For each node, an infection time distribution is computed as a BP marginal and the mean and standard deviation of this distribution are plotted against the true time; along with the inferred probability of being the source of the infection. The plot shows large correlation between true and inferred infection times, and also that the true origin (that was not observed) corresponds to the individual with largest inferred probability.

Finally, the proposed approach can be also used to estimate the epidemic parameters. Indeed, the partition function  $Z$  in (3) is proportional to the likelihood of the unknown parameters. The log-likelihood  $\log Z$  is well-approximated

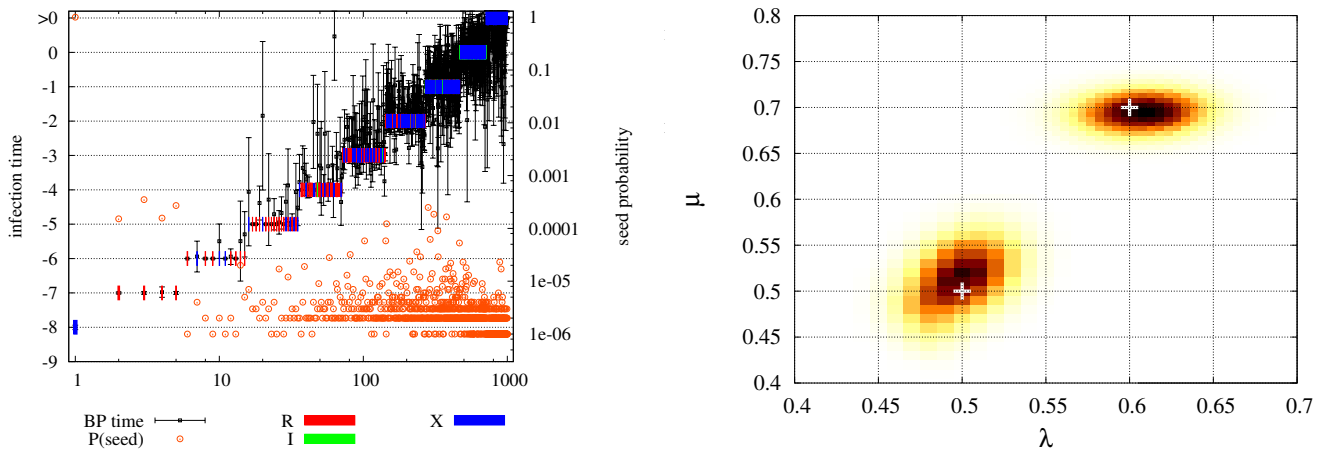


Figure 3. (Color online) Examples of inference with incomplete information on a RRG with  $N = 1000$ ,  $k = 4$ , from observations at time  $T = 0$  on an epidemic with  $T_0 = -8$  (unknown to BP). Left: inference of an epidemic with  $\lambda = 0.7$ ,  $\mu = 0.6$  with prior seed probability  $10^{-6}$ , from observations on a fraction  $1 - \xi = 0.6$  of the nodes. Each point in the x axis corresponds to a vertex on the graph. Nodes are ordered by their real infection time (blocks, R=recovered, I=infected and X=unknown). The mean and standard deviation of their BP posterior marginal distribution of infection time is plotted (black dots and error bars) along with the marginal posterior probability of self-infection (orange, circles, right axis). Note that the correct origin is correctly detected, even if it was not observed. Right: Inference of epidemic parameters. The heat-plot shows the estimation of the likelihood density of the parameters for two virtual epidemics with parameters  $\lambda = 0.7$  and  $\mu = 0.6$  and epidemic age  $T - T_0 = 8$ , and  $\lambda = 0.5$  and  $\mu = 0.5$  and  $T - T_0 = 10$ . In this realizations the epidemics involved 653 and 462 nodes of the graph respectively. The time  $T_0$  was not known to the BP algorithm. The inferred maximum for the log-likelihood (minimum of the free energy) was  $\hat{\lambda} = 0.695$ ,  $\hat{\mu} = 0.605$  for the first and  $\hat{\lambda} = 0.5$  and  $\hat{\mu} = 0.52$  for the second epidemic.

by the opposite of the Bethe free energy, which can be computed easily as a function of BP messages on a fixed point (see SM). We show this scheme in action in two different realizations of epidemics with parameters  $\lambda = 0.7$ ,  $\mu = 0.6$  and epidemic age  $T - T_0 = 8$ , and  $\lambda = 0.5$ ,  $\mu = 0.5$  and  $T - T_0 = 10$ , in Figure 3. In both cases we do not provide BP with the epidemic age. BP equations are iterated for every pair of  $(\mu, \lambda)$ , and the resulting Bethe free energy is computed after convergence. The point with the highest likelihood is  $\hat{\lambda} = 0.695$  and  $\hat{\mu} = 0.605$  for the first, and  $\hat{\lambda} = 0.5$  and  $\hat{\mu} = 0.52$  for the second epidemics. In both cases the epidemic age and the zero patient are correctly inferred.

## VI. INFERENCE OF MULTIPLE SOURCES.

If the origin of the epidemic is not a single source, but a set of sources, methods based on the exhaustive exploration of initial states like DMP suffer a combinatorial explosion. This problem does not affect BP, as the trace over initial conditions is performed directly within the framework. We show in Fig. 4 experiments with multiple seeds, showing that effective inference can also be achieved in this regime.

## VII. DYNAMICALLY EVOLVING NETWORKS.

A richer representation of the interactions of individuals can involve dynamic networks, in which the presence or the intensity of the contact among nodes vary over time. This situation can be modeled by means of time-dependent transmission probabilities  $\lambda_{ij}$ . In our framework, such a dynamic scenario can be analyzed by introducing an explicit dependency of the distribution of transmission delays on the infection times  $t_i$ , i.e.  $\omega_{ij} = \omega_{ij}(s_{ij}|g_i, t_i)$  (see details in SM). We considered the interesting dataset [9], corresponding to a large list of time-stamped face-to-face 20 seconds contacts between couples of visitors in a cultural event, obtained using badges with RFID technology. The dataset is separated into days (visitors in different days are disjoint). We aggregated the 20 second resolution of the data for a given day into  $T$  effective time steps, and simulated the progression of a virtual epidemic initiated by a random visitor. We employed the following set of parameters: probability of contagion in a 20 second interval  $\lambda_{ij}^{20s} = 0.1$ , recovery probability  $\mu = 0.1$ , and  $T - T_0 = 30$ . We focused on the known initial time scenario  $T_0 = 0$ , because this corresponds to the situation in which the epidemic is introduced from the outside by an individual who was infected before entering

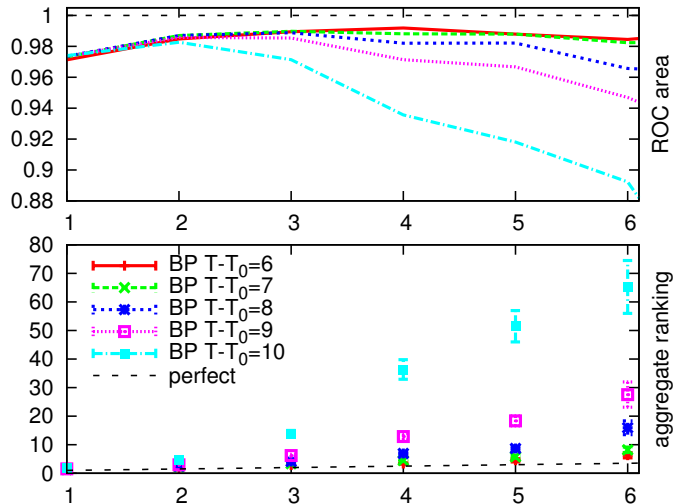


Figure 4. Inference of multiple seeds on 1 000 virtual epidemics with  $\mu = 1, \lambda = 0.5$ , seed probability 0.002 and different observation times  $T - T_0$  (unknown to the inference algorithm). Bottom: average sum of the rankings of the true seeds in the inferred order is plotted vs. the true number of seeds. Top: the average normalized mean ranking, that equals the average area of the ROC curve. Each ROC curve was computed restricted to the epidemic subgraph.

the facilities, and concentrated on the last four days of the event in which the number of individuals and interactions was generally larger. We simulated 2000 random epidemics with the above parameters, and kept the 50 epidemics with larger number of infected individuals ( $98 \pm 14$ ). The correct origin was identified perfectly in 13 cases (26%), and in general its normalized ranking  $(Rank\ i_0)/|I + R|$  was in average  $0.07 \pm 0.11$ . Finally, also infection times were recovered with good accuracy: the probability assigned to the correct infection time (for infected individuals) was in average  $0.53 \pm 0.06$ , and the average absolute error in the inferred infection time step was  $0.76 \pm 0.23$ , corresponding to about 12 minutes of real time.

### VIII. CONCLUSIONS.

We introduced a systematic, consistent and computationally efficient approach to the calculation of posterior distributions and likelihood of model parameters for a broad class of epidemic models. Besides providing the exact solution for acyclic graphs, we have shown the approach to be extremely effective also for synthetic and real networks with cycles, both in a static and a dynamic context. More general epidemic models such as the Reed-Frost model [10] that include latency and incubation times, can be analyzed by simply defining appropriate recovery  $\mu_i$  and transmission probabilities  $\lambda_{ij}$  that depend on the time after infection and by employing stochastic observation laws  $\zeta_i$ . This generalizations can be incorporated in the BP formalism in a straightforward way.

### IX. ACKNOWLEDGMENTS.

The authors acknowledge the European Grants FET Open No. 265496 and ERC No. 267915 and Italian FIRB Project No. RBFR10QUW4.

### Appendix A: Belief propagation equations

We show the derivation of the Belief Propagation equations (also known as *replica-symmetric cavity equations* in statistical physics) for the posterior distribution of the SIR model in (3):

$$\psi_i \left( t_i, g_i, \left\{ \left( t_i^{(j)}, t_j'^{(j)}, g_i^{(j)} \right) \right\}_{j \in \partial i} \right) = \left( \delta(t_i, 0) + \delta \left( t_i, \left( 1 + \min_{j \in \partial i} \{ t_j'^{(j)} \} \right) \right) \right) \prod_{j \in \partial i} \delta(g_i, g_i^{(j)}) \delta(t_i, t_i^{(j)}) \quad (\text{A1})$$

$$\phi_{ij} \left( (t_i, t_j', g_i), (t_j, t_i', g_j) \right) = \omega_{ij} (t_i' - t_i | g_i) \omega_{ji} (t_j' - t_j | g_j) \quad (\text{A2})$$

$$\gamma_i(t_i) = \gamma \delta(t_i, 0) + (1 - \gamma)(1 - \delta(t_i, 0)) \quad (\text{A3})$$

$$\zeta_i(t_i, g_i, x_i^T) = \mathbb{1}[x_i^T = I, t_i \leq T < t_i + g_i] + \mathbb{1}[x_i^T = S, T < t_i + g_i] + \quad (\text{A4})$$

$$+ \mathbb{1}[x_i^T = R, t_i + g_i \leq T] \quad (\text{A5})$$

$$\mathcal{G}_i(g_i) = r_i(1 - r_i)^{g_i} \quad (\text{A6})$$

Belief propagation consists in a set of equations for single-site probability distributions labeled by directed graph edges. These equations are solved by iteration, and on a fixed point give an approximation for single-site marginals and other quantities of interest like the partition function  $Z$ .

We recall the general form of the BP equations in the following. For a factorized probability measure on  $\underline{z} = \{z_i\}$ ,

$$M(\underline{z}) = \frac{1}{Z} \prod_a F_a(\underline{z}_a) \quad (\text{A7})$$

where  $\underline{z}_a$  is the subvector of variables that  $F_a$  depends on, the general form of the equations is

$$p_{F_a \rightarrow i}(z_i) = \frac{1}{z_{ai}} \sum_{\{z_j: j \in \partial a \setminus i\}} F_a(\{z_i\}_{i \in \partial a}) \prod_{j \in \partial a \setminus i} m_{j \rightarrow F_a}(z_j) \quad (\text{A8})$$

$$m_{i \rightarrow F_a}(z_i) = \frac{1}{z_{ia}} \prod_{b \in \partial i \setminus a} p_{F_b \rightarrow i}(z_i) \quad (\text{A9})$$

$$m_i(z_i) = \frac{1}{z_i} \prod_{b \in \partial i} p_{F_b \rightarrow i}(z_i) \quad (\text{A10})$$

where  $F_a$  is a *factor* (i.e.  $\psi_i$ ,  $\phi_{ij}$ ,  $\gamma_i$ ,  $\zeta_i$  or  $\mathcal{G}_i$  in our case),  $z_i$  is a *variable* (i.e.  $(t_i, g_i), (t_i^{(j)}, t_j'^{(j)}, g_i^{(j)})$  in our case),  $\partial a$  is the subset of indices of variables in factor  $F_a$  and  $\partial i$  is the subset of factors that depend on  $z_i$ . Terms  $z_{ia}, z_{ai}$  and  $z_i$  are normalization factors that can be calculated once the rest of the right-hand side is computed. While equations (A9)-(A10) can be always computed efficiently in general, the computation of trace in (A8) may need a time which is exponential in the number of participating variables. Update equations (A8) for factors  $\phi_{ij}$ ,  $\gamma_i$ ,  $\zeta_i$  and  $\mathcal{G}_i$  can be computed in a straightforward way because they involve a very small (constant) number of variables each. We show the derivation of an efficient version of equation (A8) for factor  $\psi_i$  that can be computed in linear time in the degree of vertex  $i$ :

$$p_{\psi_i \rightarrow j} \left( t_i^{(j)}, t_j^{(j)}, g_i^{(j)} \right) \propto \sum_{g_i, t_i} \sum_{\left\{ t_i^{(k)}, t_k^{(k)}, g_i^{(k)} \right\}} m_{i \rightarrow \psi_i} (t_i, g_i) \times \quad (\text{A11})$$

$$\times \prod_{k \in \partial i \setminus j} m_{k \rightarrow \psi_i} \left( t_i^{(k)}, t_k^{(k)}, g_i^{(k)} \right) \psi_i \left( t_i, g_i, \left\{ \left( t_i^{(j)}, t_j^{(j)}, g_i^{(j)} \right) \right\}_{j \in \partial i} \right) \\ \propto \sum_{g_i^{(j)}, t_i^{(j)}} m_{i \rightarrow \psi_i} \left( t_i^{(j)}, g_i^{(j)} \right) \sum_{\left\{ t_k^{(k)} \right\}} \prod_{k \in \partial i \setminus j} m_{k \rightarrow \psi_i} \left( t_i^{(k)}, t_k^{(k)}, g_i^{(k)} \right) \times \quad (\text{A12})$$

$$\times \left( \delta(t_i, 0) + \delta \left( t_i, \left( 1 + \min_{j \in \partial i} \left\{ t_j^{(j)} \right\} \right) \right) \right) \\ \propto \delta \left( t_i^{(j)}, 0 \right) m_{i \rightarrow \psi_i} \left( 0, g_i^{(j)} \right) \left\{ \prod_{k \in \partial i \setminus j} \sum_{t_k^{(k)}} m_{k \rightarrow \psi_i} \left( 0, t_k^{(k)}, g_i^{(j)} \right) + \right. \quad (\text{A13})$$

$$\left. + \sum_{\left\{ t_k^{(k)} \right\}} \prod_{k \in \partial i \setminus j} m_{k \rightarrow \psi_i} \left( t_i^{(j)}, t_k^{(k)}, g_i^{(j)} \right) \delta \left( t_i^{(j)}, \left( 1 + \min_{k \in \partial i} \left\{ t_k^{(k)} \right\} \right) \right) \right\} \\ = \delta \left( t_i^{(j)}, 0 \right) m_{i \rightarrow \psi_i} \left( 0, g_i^{(j)} \right) \prod_{k \in \partial i \setminus j} \sum_{t_k^{(k)}} m_{k \rightarrow \psi_i} \left( 0, t_k^{(k)}, g_i^{(j)} \right) + \quad (\text{A14})$$

$$+ m_{i \rightarrow \psi_i} \left( t_i^{(j)}, g_i^{(j)} \right) \mathbb{1} \left( t_i^{(j)} \leq t_j^{(j)} + 1 \right) \prod_{k \in \partial i \setminus j} \sum_{t_k^{(k)} \geq t_i^{(j)} - 1} m_{k \rightarrow \psi_i} \left( t_i^{(j)}, t_k^{(k)}, g_i^{(j)} \right) \\ - m_{i \rightarrow \psi_i} \left( t_i^{(j)}, g_i^{(j)} \right) \mathbb{1} \left( t_i^{(j)} < t_j^{(j)} + 1 \right) \prod_{k \in \partial i \setminus j} \sum_{t_k^{(k)} > t_i^{(j)} - 1} m_{k \rightarrow \psi_i} \left( t_i^{(j)}, t_k^{(k)}, g_i^{(j)} \right)$$

where in (A14) we use the fact that  $\delta \left( t_i, \left( 1 + \min_{j \in \partial i} \left\{ t_j^{(j)} \right\} \right) \right) = \prod_{j \in \partial i} \mathbb{1} \left( t_i \leq t_j^{(j)} + 1 \right) - \prod_{j \in \partial i} \mathbb{1} \left( t_i < t_j^{(j)} + 1 \right)$ . The last equation (A14) can be computed efficiently. Similarly,

$$p_{\psi_i \rightarrow i} (t_i, g_i) \propto \delta(t_i, 0) \prod_{k \in \partial i} \sum_{t_k^{(k)}} m_{k \rightarrow \psi_i} \left( 0, t_k^{(k)}, g_i \right) + \quad (\text{A15}) \\ + \prod_{k \in \partial i} \sum_{t_k^{(k)} \geq t_i - 1} m_{k \rightarrow \psi_i} \left( t_i, t_k^{(k)}, g_i \right) \\ - \prod_{k \in \partial i} \sum_{t_k^{(k)} > t_i - 1} m_{k \rightarrow \psi_i} \left( t_i, t_k^{(k)}, g_i \right)$$

A more efficient parametrization of the equations can be derived by noting that in the right-hand side of (A14), incoming distributions  $m_{i \rightarrow \psi_i}$  are aggregated in a simple way. In this way the BP update of  $\psi_i$  can be computed in time  $O(G \cdot T \cdot |\partial i|)$ , where  $G$  is the maximum allowed recovery delay, and the one of  $\phi_{ij}$  in time  $O(G^2 \cdot T)$ . In practice,  $G$  can be taken constant for a geometric distribution  $\mathcal{G}$ . A single BP iteration can be thus computed in time  $O(T \cdot G^2 \cdot |E|)$ . We remark that the BP equations for the posterior distribution are exact (and have a unique solution) on tree factor graphs [11]. As the topology of the factor graph mirrors the one of the original graph, (3) allows the exact computation of posterior marginals for the SIR model on tree graphs (at difference with the DMP method).

## Appendix B: Bethe Free Energy

The cavity scheme allows one to compute approximately the Free Energy of the system  $f = -\log Z$ . In our case,  $\log Z$  corresponds to the log-likelihood of external parameters, and thus can be used to estimate them. One of the many expressions of the Bethe free energy as a function of BP messages and their normalizations has the following form (see e.g. [12]):

$$-f = \sum_a f_a + \sum_i f_i - \sum_{ia} f_{ia} \quad (\text{B1})$$



where

$$f_a = \log \left( \frac{1}{|\partial a|} \sum_{i \in \partial a} z_{ai} \sum_{z_i} p_{F_a \rightarrow i}(z_i) \cdot m_{i \rightarrow F_a}(z_i) \right) \quad (\text{B2})$$

$$f_{ia} = \log \left( \sum_{z_i} p_{F_a \rightarrow i}(z_i) m_{i \rightarrow F_a}(z_i) \right) \quad (\text{B3})$$

$$f_i = \log \left( \sum_{z_i} \prod_{i \in a} p_{F_a \rightarrow i}(z_i) \right) \quad (\text{B4})$$

### Appendix C: Dynamically evolving networks

To cope with time dependent transmission probabilities, it suffices to consider transmission delay probabilities that depend on  $t_i$ , i.e.  $\omega_{ij}(s_i|g_i, t_i) = \lambda_{ij}(t_i) \prod_{t=0}^{t_i-1} (1 - \lambda_{ij}(t_i))$  for  $s_i \leq g_i$  and  $\omega_{ij}(\infty|g_i, t_i) = 1 - \sum_{s=0}^{g_i} \omega_{ij}(s|g_i, t_i)$ , the rest of the formalism remaining the same. We studied the case of dynamically evolving networks, in which the transmission probability  $\lambda_{ij}$  depends on time (representing the time-evolution of interactions between agents). For this purpose, we employed the interesting dataset [9], corresponding to a large list of time-stamped face-to-face 20 seconds contacts between couples of visitors in a cultural event, obtained using badges with RFID technology. The dataset is separated into days (visitors in different days are disjoint). We aggregated the 20 second resolution of the data for a given day into  $T$  effective time steps, and simulated the progression of a virtual epidemic initiated by a random visitor. We employed the following set of parameters: probability  $\lambda_{ij}^{20s} = 0.1$  of contagion in a 20 second interval, recovery probability  $\mu = 0.1$ , and  $T - T_0 = 30$ . We focused on the known-time setup (at the start of the day), because this corresponds to the situation in which the epidemic is introduced from the outside by an individual who was infected before entering the facilities (the patient zero). We concentrated on the last four days of the event in which the number of individuals and interactions was generally larger. We simulated 2000 random epidemics with the above parameters, and attempted inference on the largest 50 in terms of number of infected plus recovered individuals (all occurred on two of the four days). The results are summarized in Table I.

### Appendix D: Dynamic Message Passing

Dynamic message passing (DMP) [5] attempts the inference of the zero patient in the following way. First, Bayes' theorem suggests that the desired probability  $P(i|\mathbf{x}^T)$  of the seed being site  $i$  given an observation  $\mathbf{x}^T$  of an epidemic at time  $T$ , is proportional to  $P(\mathbf{x}^T|i)$ . Then DMP considers an approximation of this latter probability in a factorized form:

$$P(\mathbf{x}^T|i) \simeq \prod_k P^k(x_k^T|T, i) \quad (\text{D1})$$

$$= \prod_{k|x_k^T=S} P_S^k(T, i) \prod_{l|x_l^T=I} P_I^l(T, i) \prod_{m|x_m^T=R} P_R^m(T, i). \quad (\text{D2})$$

In this expression  $P_S^k(T, i)$  ( $P_I^l(T, i)$ ,  $P_R^m(T, i)$ ) is the probability that site  $k$  ( $l, m$ ) is found in the susceptible (infected, recovered) state at observation time  $T$  if the epidemic started at site  $i$ . Note that  $P_S^k(T, i)$ ,  $P_I^l(T, i)$  and  $P_R^m(T, i)$  are probabilities in the subindex  $S, I, R$  and not in  $i$  or  $T$ . In the first line we keep the notation used in [5].

The actual values of  $P_S^k(T, i)$ ,  $P_I^l(T, i)$  and  $P_R^m(T, i)$  are obtained by iterating the forward propagation equations [6] of the SIR model, starting from node  $i$  in the graph. For each possible origin an energy-like function can be defined as  $E(i) = -\log P(\mathbf{x}^T|i)$ , and the most probable seed is therefore the one with lowest energy.

In the standard dynamic message passing approach [5], the forward equations for each possible origin are propagated over all nodes in the graph, to compute the terms  $P_S^k(T, i)$ ,  $P_I^l(T, i)$  and  $P_R^m(T, i)$ . This includes those nodes that are not participating in the actual epidemic (susceptible nodes at observation time). A restricted version of DMP can be implemented by only iterating the equations [6] over the connected component of nodes that do participate in the observed epidemic. This means that any node of the graph that is susceptible and is surrounded by susceptible nodes at observation time  $T$  is effectively removed from the DMP equations. In this way the contributions to the probabilities  $P_S^k(T, i)$ ,  $P_I^l(T, i)$  and  $P_R^m(T, i)$  come only from epidemic paths that are consistent with the observed epidemic. In other words, the effective graph for the epidemic transmission is only the part of the original graph that got infected, and its boundary. The susceptible boundary is not used in the message passing procedure, but it

| date       | origin    | size | rank | rank / size | prob(t) | dist   | date       | origin    | size | rank | rank / size | prob(t) | dist   |
|------------|-----------|------|------|-------------|---------|--------|------------|-----------|------|------|-------------|---------|--------|
| 2009/07/15 | 95158439  | 146  | 1    | 0.0068      | 0.5806  | 0.5826 | 2009/07/15 | 78119048  | 94   | 1    | 0.0106      | 0.5755  | 0.8046 |
| 2009/07/14 | 77922454  | 126  | 6    | 0.0476      | 0.4660  | 0.7763 | 2009/07/14 | 98631832  | 94   | 3    | 0.0319      | 0.4505  | 0.7595 |
| 2009/07/14 | 103350288 | 125  | 1    | 0.0080      | 0.5391  | 0.6333 | 2009/07/14 | 72744982  | 94   | 3    | 0.0319      | 0.5002  | 0.7578 |
| 2009/07/15 | 78577817  | 124  | 2    | 0.0161      | 0.6058  | 0.5766 | 2009/07/15 | 85655568  | 93   | 1    | 0.0108      | 0.6523  | 0.5071 |
| 2009/07/15 | 101974031 | 118  | 2    | 0.0169      | 0.5552  | 0.6049 | 2009/07/14 | 92864531  | 93   | 1    | 0.0108      | 0.5588  | 0.6320 |
| 2009/07/15 | 89325583  | 117  | 8    | 0.0684      | 0.5209  | 1.2151 | 2009/07/14 | 83034287  | 93   | 2    | 0.0215      | 0.5135  | 0.7246 |
| 2009/07/15 | 93192213  | 115  | 2    | 0.0174      | 0.6071  | 0.5426 | 2009/07/14 | 80150715  | 92   | 13   | 0.1413      | 0.4906  | 0.7452 |
| 2009/07/14 | 101843108 | 114  | 8    | 0.0702      | 0.4586  | 0.8525 | 2009/07/14 | 73597113  | 92   | 3    | 0.0326      | 0.4809  | 0.8183 |
| 2009/07/15 | 94961692  | 112  | 29   | 0.2589      | 0.5295  | 0.7060 | 2009/07/15 | 73597117  | 91   | 1    | 0.0110      | 0.6858  | 0.3881 |
| 2009/07/14 | 74317990  | 112  | 5    | 0.0446      | 0.4516  | 0.8683 | 2009/07/14 | 90505398  | 90   | 1    | 0.0111      | 0.5555  | 0.6216 |
| 2009/07/15 | 98631834  | 111  | 9    | 0.0811      | 0.5813  | 0.5660 | 2009/07/15 | 89325582  | 89   | 2    | 0.0225      | 0.6690  | 0.4911 |
| 2009/07/14 | 73597113  | 106  | 1    | 0.0094      | 0.4675  | 0.8319 | 2009/07/14 | 80150715  | 89   | 6    | 0.0674      | 0.4932  | 0.9085 |
| 2009/07/15 | 89325583  | 105  | 1    | 0.0095      | 0.6056  | 0.6065 | 2009/07/14 | 75694101  | 88   | 1    | 0.0114      | 0.4968  | 0.7047 |
| 2009/07/15 | 77922457  | 101  | 11   | 0.1089      | 0.5347  | 0.7624 | 2009/07/14 | 86769684  | 87   | 5    | 0.0575      | 0.4924  | 0.7301 |
| 2009/07/14 | 84476071  | 101  | 3    | 0.0297      | 0.5010  | 0.7198 | 2009/07/14 | 77267113  | 87   | 3    | 0.0345      | 0.5013  | 0.7972 |
| 2009/07/15 | 75235330  | 100  | 16   | 0.1600      | 0.5595  | 1.8555 | 2009/07/15 | 88997933  | 84   | 10   | 0.1190      | 0.5255  | 0.7626 |
| 2009/07/15 | 105512965 | 100  | 74   | 0.7400      | 0.4999  | 0.7840 | 2009/07/14 | 102695092 | 84   | 2    | 0.0238      | 0.4835  | 0.8264 |
| 2009/07/14 | 77922454  | 100  | 3    | 0.0300      | 0.5239  | 0.6433 | 2009/07/15 | 104464399 | 83   | 16   | 0.1928      | 0.5494  | 0.7205 |
| 2009/07/14 | 102301708 | 100  | 8    | 0.0800      | 0.5030  | 0.7407 | 2009/07/14 | 98631832  | 83   | 2    | 0.0241      | 0.5101  | 0.6405 |
| 2009/07/15 | 74776741  | 98   | 1    | 0.0102      | 0.6529  | 0.4721 | 2009/07/14 | 90636461  | 83   | 11   | 0.1325      | 0.4670  | 0.8715 |
| 2009/07/15 | 97124354  | 97   | 8    | 0.0825      | 0.5755  | 0.8112 | 2009/07/14 | 83886089  | 82   | 11   | 0.1341      | 0.5239  | 0.7203 |
| 2009/07/14 | 78577814  | 96   | 1    | 0.0104      | 0.5380  | 0.6256 | 2009/07/15 | 104333461 | 81   | 5    | 0.0617      | 0.5942  | 0.6730 |
| 2009/07/14 | 73597113  | 96   | 5    | 0.0521      | 0.4631  | 0.9350 | 2009/07/14 | 96075954  | 81   | 22   | 0.2716      | 0.4394  | 1.3069 |
| 2009/07/14 | 100859937 | 96   | 4    | 0.0417      | 0.5298  | 0.7131 | 2009/07/14 | 95485968  | 81   | 3    | 0.0370      | 0.4644  | 1.1777 |
| 2009/07/15 | 93192214  | 95   | 3    | 0.0316      | 0.5467  | 0.8537 | 2009/07/14 | 83820566  | 81   | 1    | 0.0123      | 0.5333  | 0.8249 |

Table I. Inference for the 50 largest virtual epidemics out of a set of 2000 simulated ones on the dataset of real timed face-to-face interactions described in ref. [9]. The second column is the label of the initially infected individual, the third column is the epidemic size, i.e.  $|I| + |R|$ , the fourth column corresponds to the rank assigned to the true origin, the fifth column is the normalized rank (i.e. the fraction of the two last columns), the sixth column reports the average over infected nodes of the probability assigned by BP to the true infection time, i.e.  $(|I| + |R|)^{-1} \sum_{i:t_i^* < \infty} P_i^{BP}(t_i^*)$  where  $t_i^*$  is the true infection time of node  $i$ , and finally the last column is the per-individual average infection time error, defined as  $(|I| + |R|)^{-1} \sum_{i:t_i^* < \infty} \sum_{t_i} P_i^{BP}(t_i) |t_i - t_i^*|$ . Note that a value of 1 (corresponding to an error of a single discrete time-step) is equivalent to about 16 minutes in real time.

is evaluated in the first factor of equation D2. In the case in which there are unobserved nodes, they are logically considered as possible infected/recovered nodes and, therefore, the DMP equations are iterated over the connected component of infected, recovered and unobserved nodes. We found that this approach, that we will call Restricted Dynamic Message Passing (DMP<sub>r</sub>), in many situations gives better estimates, as is shown in Fig. 4 of the manuscript, and also in figures 5, 6 and 7.

Despite this improvement, DMP<sub>r</sub> is still less accurate than BP. Figures 5, 6 and 7 show three sets of parameters as benchmarks. In all cases the observation time is known, and epidemics were generated with only one seed. We found that the belief propagation equations sometimes do not converge when the epidemic becomes large compared to the size of the graph (see Figs. 6 and 7). For small observation times ( $T = 5$  in Fig. 5) the epidemic remains small and BP always converges. The lack of convergence is associated to a decrease in accuracy and it is in this region where our algorithm performs worse. It is important to underline that the amount of information concerning the origin of an epidemic is reduced when the epidemic covers almost all the supporting graph, and not surprisingly all algorithms perform worse in this region (as in Fig. 6).

## Appendix E: Inference of epidemic parameters with BP and DMP

Among the methods tested in this Letter, Jordan centrality is the least effective, but is also the least demanding in terms of prior information. As presented so far, both Dynamic Message Passing and Belief Propagation require not

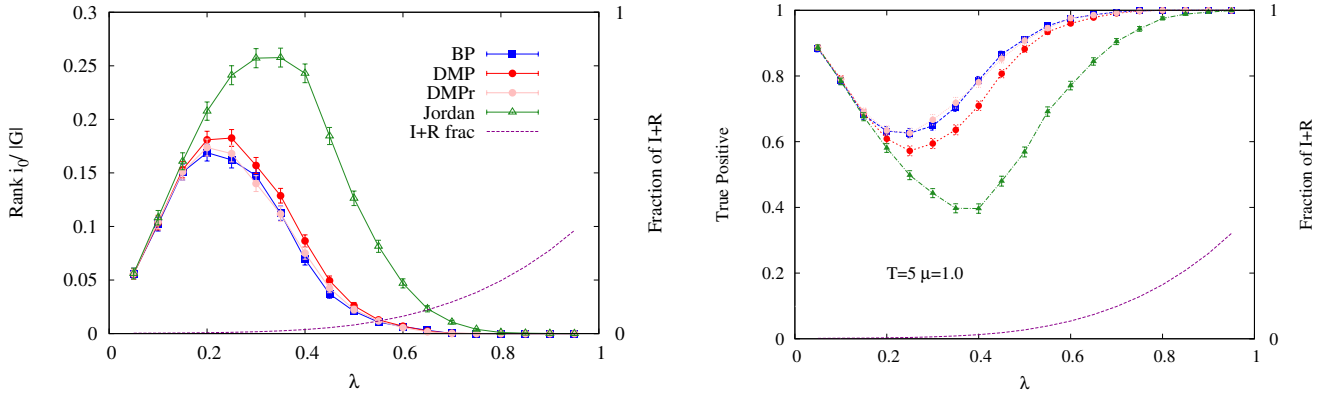


Figure 5. **Left:** Relative ranking of the true zero patient with respect to the size of the epidemic, as a function of the transmission probability  $\lambda$ . The size of the epidemic is shown as a dashed line, and corresponds to the right y axis. **Right:** Fraction of the instances in which the true zero patient is found by each algorithm. The forward epidemic is propagated until observation time  $T = 5$ , with recovery probability  $\mu = 1$ . Simulations were run over 1000 samples of random regular graphs with  $N = 1000$  and degree 4.

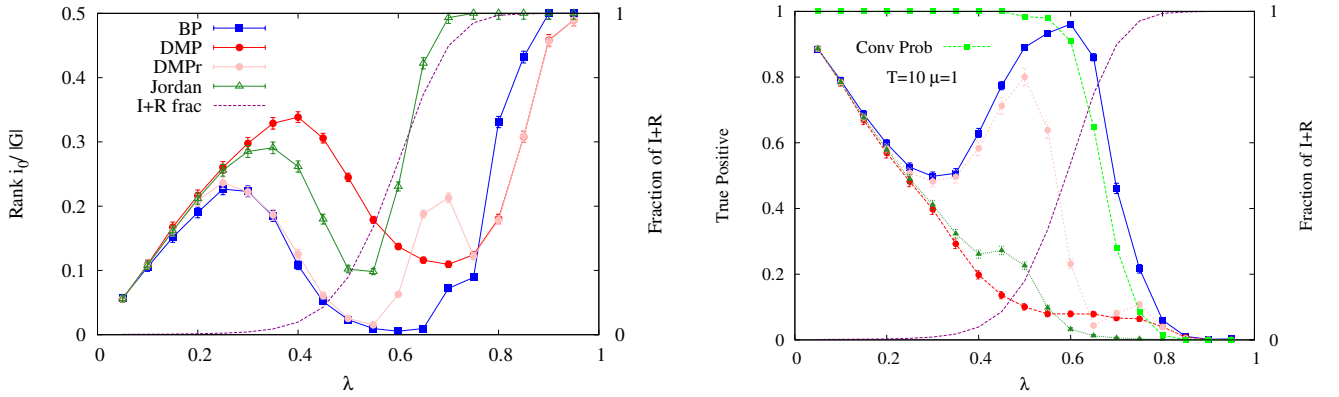


Figure 6. **Left:** Relative ranking of the true zero patient with respect to the size of the epidemic, as a function of the transmission probability  $\lambda$ . The size of the epidemic is shown as a dashed line, and corresponds to the right y axis. **Right:** Fraction of the instances in which the true zero patient is found by each algorithm. The forward epidemic is propagated until observation time  $T = 10$ , with recovery probability  $\mu = 1$ . Simulations were run over 1000 samples of random regular graphs with  $N = 1000$  and degree 4.

only the network of contacts, but also the values of the transmission probability  $\lambda_{ij}$ , and the recovery probability  $\mu_i$ . At least in the case of homogeneous parameters  $\lambda_{ij} \equiv \lambda, \mu_i \equiv \mu$ , this requirement can be relaxed since both methods can be used to infer the epidemic parameters by comparing the energy or the free energy obtained for different pairs  $(\lambda, \mu)$ . The probability of parameters  $(\lambda, \mu)$  given an observation of an epidemic is

$$P(\lambda, \mu | \mathbf{x}^T) = \frac{P(\mathbf{x}^T | \lambda, \mu) P(\lambda, \mu)}{P(\mathbf{x}^T)} \propto P(\mathbf{x}^T | \lambda, \mu) \quad (\text{E1})$$

assuming a uniform prior for  $(\lambda, \mu)$ .

### Inference with Dynamic Message Passing

The DMP method gives a probability to the observed epidemic starting from every single possible seed,  $P(\mathbf{x}^T | i, \lambda, \mu)$  (see (D2)), so we can write

$$P(\mathbf{x}^T | \lambda, \mu) = \sum_i P(\mathbf{x}^T | i, \lambda, \mu) \quad (\text{E2})$$

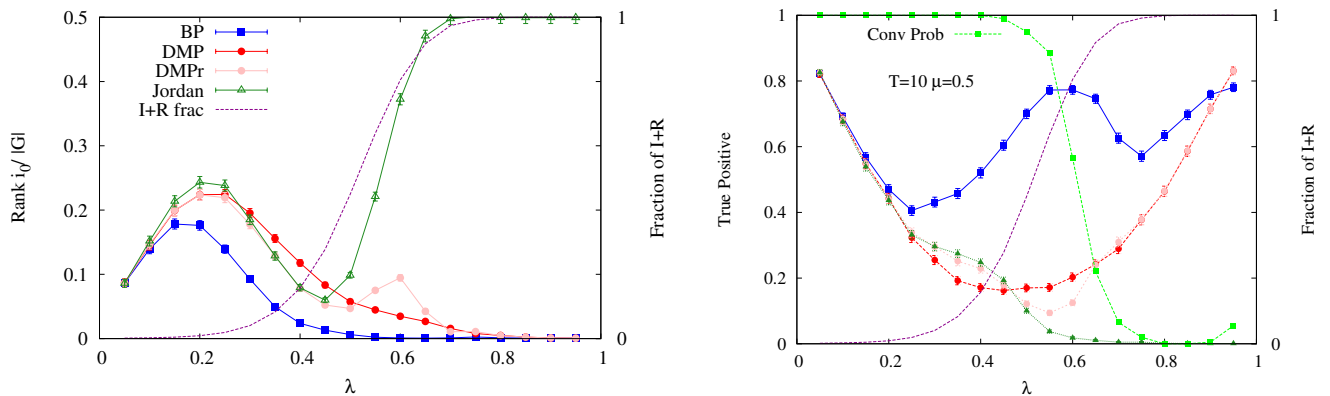


Figure 7. **Left:** Relative ranking of the true zero patient with respect to the size of the epidemic, as a function of the transmission probability  $\lambda$ . The size of the epidemic is shown as a dashed line, and corresponds to the right y axis. **Right:** Fraction of the instances in which the true zero patient is found by each algorithm. The forward epidemic is propagated until observation time  $T = 10$ , with recovery probability  $\mu = 0.5$ . The figure in the right corresponds to the one shown in the manuscript as Fig 2, but with a different parameterization of the x axis. Simulations were run over 1000 samples of random regular graphs with  $N = 1000$  and degree 4.

An estimate of the negated log-likelihood of the parameters can therefore be given as the DMP free energy

$$f_{\text{DMP}}(\lambda, \mu) = -\log P(\lambda, \mu | \mathbf{x}^T) \simeq -\log \sum_i P(\mathbf{x}^T | i, \lambda, \mu). \quad (\text{E3})$$

We call this a free energy since the last expression can be written as  $-\log \sum_i \exp(-E(i))$ . The lower this free energy, the more likely the parameters.

### Inference with Belief Propagation

Following the approach of the present Letter, the posterior of the parameters can be computed as

$$\mathcal{P}(\lambda, \mu | \mathbf{x}^T) \propto \sum_{\mathbf{t}, \mathbf{g}, \mathbf{x}^0} \mathcal{P}(\mathbf{x}^T | \mathbf{t}, \mathbf{g}) \mathcal{P}(\mathbf{t}, \mathbf{g} | \mathbf{x}^0) \mathcal{P}(\mathbf{x}^0). \quad (\text{E4})$$

where the trace goes over the infection times  $\mathbf{t}$ , the recovery delays  $\mathbf{g}$  and the different choices of zero patients  $\mathbf{x}^0$ .

Therefore the desired log-likelihood of the parameters can be computed as the negated free energy of the model in (3):

$$f(\lambda, \mu) = -\log Z \quad (\text{E5})$$

where  $Z$  is given in eq. (3). The exact calculation of  $Z$  is computationally hard, but the same Bethe approximation used for the inference of  $\mathbf{x}^0$  yields an approximate  $f_{\text{BP}}(\lambda, \mu)$ , given in (B1) for the free energy of this model.

In the manuscript is presented an example of the functions  $f_{\text{DMP}}(\lambda, \mu)$  and  $f_{\text{BP}}(\lambda, \mu)$  for an epidemic observed at time  $T = 8$ . The 2-dimensional space of parameters  $(\lambda, \mu)$  is discretized and the (standardized) values of the free energies shown in a heat-plot. Note that every single point of the graph corresponds to a run of DMP and DMPr with the corresponding parameters.

- 
- [1] J. Snow, *On the mode of communication of cholera* (John Churchill, London, 1855).
  - [2] D. Shah and T. Zaman, SIGMETRICS **38**, 203–214 (2010); IEEE Trans Inf Theory **57**, 5163–5181 (2011); C. H. Comin and L. da Fontoura Costa, Phys. Rev. E **84**, 056105 (2011).
  - [3] W. Luo, W. P. Tay, and M. Leng, IEEE Trans. Signal Process. **61**, 2850 (2013); P. C. Pinto, P. Thiran, and M. Vetterli, Phys. Rev. Lett. **109**, 068702 (2012).

- [4] N. Antulov-Fantulin, A. Lancic, H. Stefancic, M. Sikic, and T. Smuc, *Statistical inference framework for source detection of contagion processes on arbitrary network structures*, arXiv e-print 1304.0018 (2013).
- [5] A. Y. Lokhov, M. Mézard, H. Ohta, and L. Zdeborová, *Inferring the origin of an epidemic with dynamic message-passing algorithm*, arXiv e-print 1303.5315 (2013).
- [6] B. Karrer and M. E. J. Newman, Phys. Rev. E **82**, 016101 (2010).
- [7] D. Kempe, J. Kleinberg, and É. Tardos, in *Proceedings of the ninth ACM SIGKDD international conference on Knowledge discovery and data mining*, KDD '03 (ACM, New York, NY, USA, 2003) p. 137–146.
- [8] F. Altarelli, A. Braunstein, L. Dall'Asta, and R. Zecchina, *Optimizing spread dynamics on graphs by message passing*, arXiv e-print 1203.1426 (2012); Phys. Rev. E **87**, 062115 (2013).
- [9] L. Isella, J. Stehlé, A. Barrat, C. Cattuto, J.-F. Pinton, and W. Van den Broeck, Journal of Theoretical Biology **271**, 166 (2011).
- [10] N. T. J. Bailey, *The mathematical theory of infectious diseases and its applications* (Griffin, London, 1975).
- [11] J. Pearl, *Reverend Bayes on inference engines: A distributed hierarchical approach* (Cognitive Systems Laboratory, School of Engineering and Applied Science, University of California, Los Angeles, 1982).
- [12] M. Mézard and A. Montanari, *Information, Physics, and Computation* (Oxford University Press, 2009).